

Phase diagram of $\text{La}_{5/8-y}\text{Nd}_y\text{Ca}_{3/8}\text{MnO}_3$ manganites

This article has been downloaded from IOPscience. Please scroll down to see the full text article.

2007 J. Phys.: Condens. Matter 19 186226

(<http://iopscience.iop.org/0953-8984/19/18/186226>)

View [the table of contents for this issue](#), or go to the [journal homepage](#) for more

Download details:

IP Address: 129.252.86.83

The article was downloaded on 28/05/2010 at 18:42

Please note that [terms and conditions apply](#).

Phase diagram of $\text{La}_{5/8-y}\text{Nd}_y\text{Ca}_{3/8}\text{MnO}_3$ manganites

J Sacanell^{1,4}, P Levy¹, A G Leyva^{1,2}, F Parisi^{1,2} and L Ghivelder³

¹ Departamento de Física, Centro Atómico Constituyentes, CNEA, Avenida General Paz 1499 (1650), San Martín, Provincia de Buenos Aires, Argentina

² Escuela de Ciencia y Tecnología, UNSAM, San Martín, Buenos Aires, Argentina

³ Instituto de Física, Universidade Federal do Rio de Janeiro, Caixa Postal 68528, Rio de Janeiro, RJ 21941-972, Brazil

E-mail: sacanell@cnea.gov.ar

Received 24 October 2006, in final form 13 February 2007

Published 13 April 2007

Online at stacks.iop.org/JPhysCM/19/186226

Abstract

We report a detailed study of the electric transport and magnetic properties of the $\text{La}_{5/8-y}\text{Nd}_y\text{Ca}_{3/8}\text{MnO}_3$ manganite system. Substitution of La^{3+} by smaller Nd^{3+} ions reduces the mean ionic radius of the A-site ion. We have studied samples in the entire range between La-rich and Nd-rich compounds ($0.1 < y < 0.625$). Results of dc magnetization and resistivity show that doping destabilizes the ferromagnetic (FM) character of the pure La compound and triggers the formation of a phase-separated state at intermediate doping. We have also found evidence of a dynamical behaviour within the phase-separated state. A phase diagram is constructed, summarizing the effect of chemical substitution on the system.

1. Introduction

Manganese-based oxides, also known as manganites, represent one of the most widely studied strongly correlated electron system since the discovery of the colossal magnetoresistance (CMR) effect [1]. A substantial amount of work has been devoted to study the low-temperature state of the manganites, characterized by the intrinsic coexistence of two or more phases on a submicrometre scale [2], a phenomenon known as phase separation (PS). This mixture is usually formed by ferromagnetic (FM) conductive and antiferromagnetic (AFM) insulating charge ordered (CO) phases [3, 4].

It is known that the substitution of La by Pr in the $\text{La}_{5/8-y}\text{Pr}_y\text{Ca}_{3/8}\text{MnO}_3$ system destabilizes the FM state in favour of the AFM CO state. This effect is attributed to the increment in the distortions on the Mn–O–Mn bonds induced by doping. The electrical and magnetic [5] and the thermal properties [6] of this system can be described within the PS scenario. In addition, several works have reported the existence of a dynamical behaviour in different manganite samples which display the phase-separation phenomena [5, 7–11]. It is

⁴ Author to whom any correspondence should be addressed.

now believed that chemical and structural disorder are the key factors for the formation of a glass-like state [12, 13].

The $\text{La}_{5/8-y}\text{Nd}_y\text{Ca}_{3/8}\text{MnO}_3$ system is a solid solution of $\text{La}_{5/8}\text{Ca}_{3/8}\text{MnO}_3$ and $\text{Nd}_{5/8}\text{Ca}_{3/8}\text{MnO}_3$, leading to a series of compounds in which the only varied parameter is the mean radius of the A-site ion. Nd ions are slightly smaller than Pr ions, so the effects related to the Mn–O–Mn distortions are expected to be enhanced. In the literature of manganites there are few reports on $\text{La}_{5/8-y}\text{Nd}_y\text{Ca}_{3/8}\text{MnO}_3$. Rao *et al* [14] studied the structural features on the $\text{La}_{(2-x)/3}\text{Nd}_{x/3}\text{Ca}_{1/3}\text{MnO}_3$ series in which they suggest the existence of La-rich metallic regions coexisting with Nd-rich semiconducting regions. A T - z phase diagram, mostly based on magnetic measurements, has already been obtained for the $(\text{La}_{1-z}\text{Nd}_z)_{1-x}\text{Ca}_x\text{MnO}_3$ system ($x = 0.45$), showing a change from a ferromagnetic metallic phase to a charge-ordered insulating phase while increasing z [15], with a scenario of coexisting phases at intermediate doping. The ground-state phase diagram in the x - z space was also presented, showing the existence of FM, CO and PS states [15]. Evidence of the phase-separated character in several compounds of the series was also found using Raman spectroscopy [16–18]. The phase-separated state induced by chemical substitution with Nd, Gd and Y was studied by Sudheendra *et al* [19]; the authors showed that disorder, related to variance of the mean radius of the A-site ion, favours the AFM phase. Regarding the dynamics of the phase-separated state, Rivadulla *et al* [20] showed that the low-temperature state constitutes a self-generated ensemble of magnetic clusters that behaves like a spin glass in $(\text{La}_{0.25}\text{Nd}_{0.75})_{0.7}\text{Ca}_{0.3}\text{MnO}_3$.

In this work we present a detailed study based on the electrical and magnetic properties of the $\text{La}_{5/8-y}\text{Nd}_y\text{Ca}_{3/8}\text{MnO}_3$ series, focusing especially on characterization of the physical response of the system within the phase-separated regime. As has been shown [11], in the PS regime strong dynamical effects are responsible for the blurring of the real equilibrium state of the system. This dynamical regime is characterized by the strong difference between the magnetization measurements in zero field cooled (ZFC) and field cooled (FC) modes and in the existence of blocking temperatures, resembling the behaviour of spin glasses [11]. We have used our data to construct the electric and magnetic phase diagram of the system, including the existence of frozen and dynamic regimes suggested by these measurements. We have paid special attention in a detailed description of the low-temperature phase-separated state corresponding to intermediate doping.

2. Experimental details

Bulk polycrystalline samples of $\text{La}_{5/8-y}\text{Nd}_y\text{Ca}_{3/8}\text{MnO}_3$ (LNCMO(y)) were synthesized following the liquid mix method (citrate polymerization). The obtained powder was pressed into bars with dimensions of $5 \times 1 \times 1 \text{ mm}^3$. The x-ray diffraction pattern corresponds to a single-phase material, with no spurious lines observed. dc magnetization measurements were performed in a Quantum Design PPMS system. Resistivity was measured in a He closed-cycle cryogenerator using the standard four-probe method.

3. Results and discussion

Figure 1 shows the dc magnetization (M) and resistivity (ρ) as a function of temperature (T) for LNCMO(y) samples with $y = 0.1, 0.2, 0.3, 0.4, 0.5$ and 0.625 . $M(T)$ was measured in the field cooled cooling (FCC) mode using an applied magnetic field of 0.2 T.

In the low-doping limit ($y = 0.1$ and 0.2), the samples exhibit paramagnetic and insulating (PI) behaviour at high temperatures. Both samples display a typical PI to FM-metallic transition on cooling below T_C , resembling the characteristics of the $\text{La}_{5/8}\text{Ca}_{3/8}\text{MnO}_3$ parent

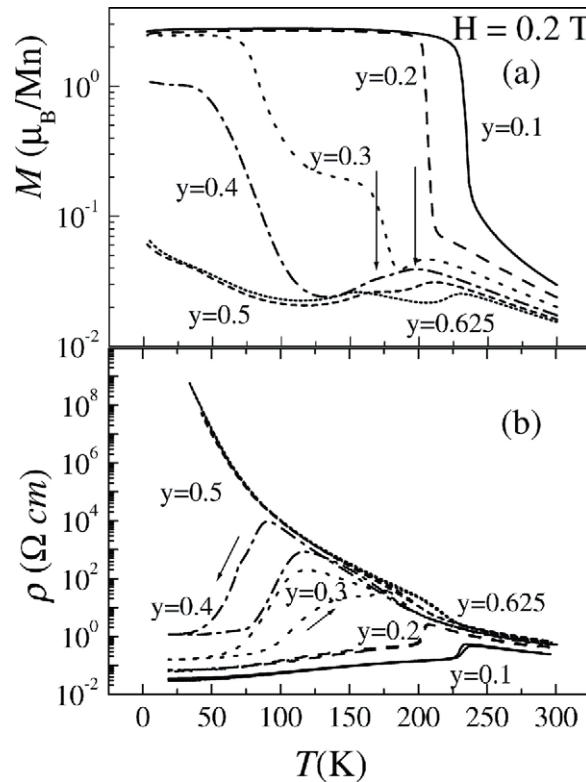


Figure 1. (a) M (FC with $H = 0.2$ T) and (b) ρ versus T for LNCMO(y) with $y = 0.1, 0.2, 0.3, 0.4, 0.5$ and 0.625 . The arrows indicate two magnetic transitions for the $y = 0.4$ sample.

compound [21]. The increment in the Nd content produces a reduction of T_C and an increase in the low-temperature resistivity, indicating that doping destabilizes the FM state. A small irreversibility is present in the ρ versus T dependence of LNCMO(0.2) around 100 K (not apparent due to the scale of the graph). Moreover, a complex behaviour is observed on both M and ρ upon further doping increase. Samples with $y = 0.3$ and 0.4 became less FM and much more resistive at low temperatures, and a clear hysteresis loop is observed in the ρ versus T dependence. On cooling, LNCMO(0.3) shows a reduction of M that is correlated with a maximum of the logarithmic derivative of the resistivity, $\partial \ln \rho / \partial (1/T)$, which indicates the arising of the CO state at $T_{co} \sim 205$ K. The onset of FM order occurs at lower temperatures, ~ 180 K, but the transition is not completed, as can be seen by the plateau in M between 100 and 175 K on cooling. This data is similar to that obtained for the $\text{La}_{5/8-y}\text{Pr}_y\text{Ca}_{3/8}\text{MnO}_3$ system [3, 5, 6] in which it has been shown to be related to PS, so this suggests that the LNCMO(0.3) compound is phase separated in the FM and CO regions between 175 and 90 K. Below $T_C \approx 90$ K, magnetization reaches almost the same value as that corresponding to the pure FM compounds ($0 < y < 0.2$) at low temperature, indicating a majority FM state in this range. This transition coincides with the change from insulator to metallic behaviour, indicated by a peak in the ρ versus T dependence at T_p .

The LNCMO(0.4) sample shows a similar behaviour, but with lower values of M and a higher resistivity at low temperatures. As a distinctive feature, this compound presents two reductions of the magnetization on cooling, indicated by vertical arrows in figure 1(a): one that

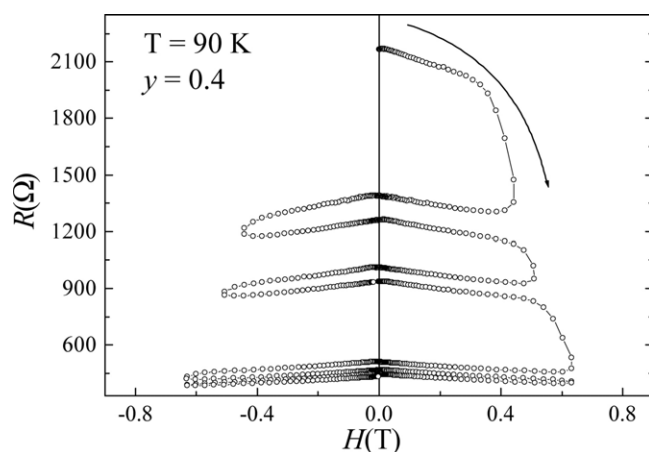


Figure 2. Resistivity as a function of the magnetic field for LNCMO(0.4) at ~ 90 K.

coincides with T_{co} and the other at $T \sim 175$ K, not correlated with any electrical transport feature. This peculiarity was attributed on the $\text{Pr}_{1-x}\text{Ca}_x\text{MnO}_3$ system to the appearance of an AFM state [22]. This sample presents an increase in the magnetization on cooling below ~ 100 K, but its low-temperature value is lower than that corresponding to a pure FM system, suggesting the coexistence of FM and non-FM phases. The resistivity for this sample also displays a maximum at T_p , which marks the transition from insulating to metallic behaviour.

The $y = 0.5$ and 0.625 samples show an insulating behaviour in the whole temperature range studied (see figure 1(b)). They are paramagnetic at high temperature and undergo a transition to a CO state at 210 and 230 K, respectively. On further cooling, both samples show a kink on the M versus T data which is presumably due to the AFM ordering within the CO phase [22]. The comparatively low magnetization value at low temperature for both compounds is an indication of a majority AFM-CO phase. On cooling below 100 K we can see that the magnetization of both samples shows a small upturn (figure 1(a)). This behaviour is similar to that corresponding to the magnetization curves obtained by Dupont *et al* for $\text{Nd}_{1-x}\text{Ca}_x\text{MnO}_3$ manganites [23]. By analysing electron spin resonance and neutron diffraction data, the authors claim that this feature can be related to the paramagnetic moment of the Nd ions within the AFM state of the Mn system.

On figure 2 we show resistivity as a function of applied field measurements, ρ versus H , at fixed $T \sim 90$ K for LNCMO(0.4). Negative magnetoresistance (MR) is observed for all magnetic fields, with two well-differentiated regimes: below 0.4 T we have the ‘classical’ MR effect due to the enhanced itinerancy of the electrons in the FM state [1], while for larger fields a change in the slope indicates a reduction of ρ related to the field-induced increase in the relative FM fraction, which is an effect that can only happen in a phase-separated system. It has been shown that the latter effect can produce a change in the resistivity and magnetization which persists after the field is turned off [24, 25]. Remarkably, this nonvolatile cumulative effect is observed while cycling and increasing the maximum field. The preceding result suggests to us that LNCMO samples with y near 0.4 exhibit PS around 90 K. The magnetic field was cycled to be sure that the nonvolatile reduction in the resistivity while turning off the field is not due to FM remanence but only related to the maximum applied magnetic field.

Detailed magnetic measurements provide further insight into the nature of the phase-separated state. The M versus H dependence for LNCMO(0.3) below T_C after ZFC from room

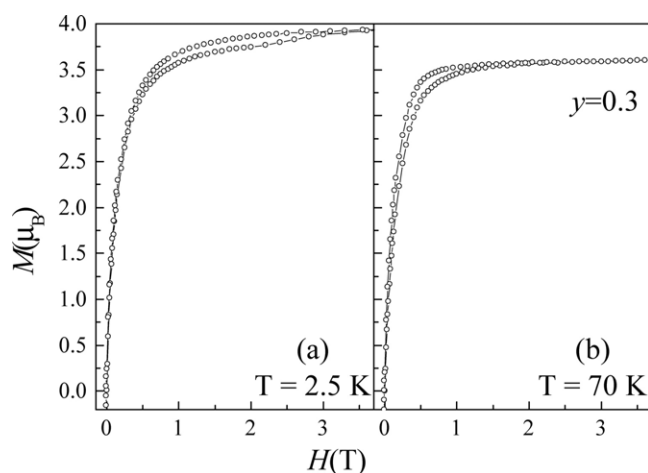


Figure 3. M versus H for LNCMO(0.3) at (a) 2.5 K and (b) 70 K.

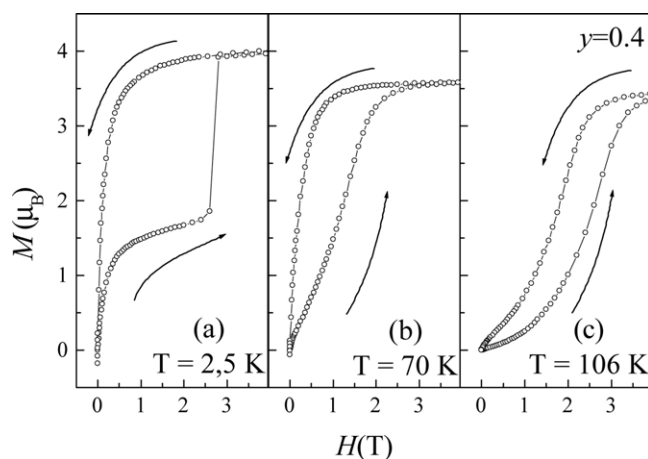


Figure 4. M versus H for LNCMO(0.4) at (a) 2.5 K, (b) 70 K and (c) 106 K. The abrupt metamagnetic transition is observed at 2.5 K for $H = 2.7$ T.

temperature is shown in figure 3. At first sight, the data show the typical shape corresponding to a soft and homogeneous FM sample. However, small traces of hysteresis signal the presence of inhomogeneities, even at temperatures well below 90 K, i.e. a phase-separated state with a majority FM fraction (see figure 1(a)). Similar measurements on LNCMO(0.4), depicted in figure 4, show the development of the phase-separated state on cooling. At 106 K we see no signature of the FM phase according to the low susceptibility near $H = 0$, while saturation can be reached just above 3 T. The existence of the FM phase at zero field is evident at $T = 70$ K and a clear hysteresis is displayed. The global behaviour at 2.5 K is qualitatively similar, with an increasing FM fraction at zero field and a irreversible metamagnetic transition due to the coexistence of FM/AFM. An interesting point is that the transition at 2.5 K is very abrupt. Similar transitions have already been observed in the $\text{La}_{5/8-y}\text{Pr}_y\text{Ca}_{3/8}\text{MnO}_3$ ($y = 0.4$) compound [26], in which the application of a large enough magnetic field can transform the low-temperature zero field cooled mostly CO state into a nearly homogeneous FM state in an

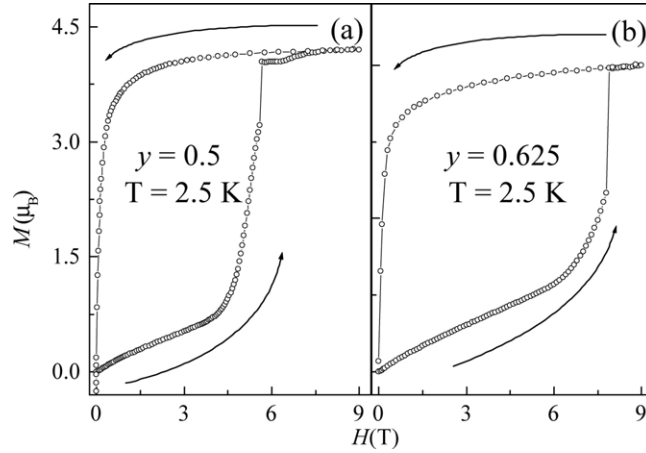


Figure 5. M versus H for (a) LNCMO(0.5) and (b) LNCMO(0.625) at 2.5 K. Abrupt metamagnetic transitions are observed at $H = 5.5$ and 7.9 T, respectively.

abrupt step-like metamagnetic transition, which remains stable even after the field is removed. The basic condition for the occurrence of the abrupt transition is that the system must reach the low-temperature regime in a strongly blocked state; the interplay between the field-induced growth of the FM phase against the CO phase and the heat released by this process seems to be the key features to explain its occurrence [26].

Figure 5 shows the M versus H dependence at 2.5 K for LNCMO(0.5) (figure 5(a)) and LNCMO(0.625) (figure 5(b)), showing no evidence of the FM phase at null H . This last data, along with the previous presented M versus T dependence for these samples, in which no transition to a FM or metallic state was found, show that the two compounds present an homogeneous AFM-CO phase for low H values. An abrupt metamagnetic transition, similar to that shown for LNCMO(0.4), is observed at around $H = 5.5$ T for LNCMO(0.5) and $H = 7.9$ T for LNCMO(0.625), indicating the existence of a blocked or frozen state at low temperature for the two compounds.

Previous studies have shown evidence of the tendency of the PS state in manganites towards a characteristic dynamic behaviour. On general grounds, when two phases coexist, competition of interactions that tend to stabilize one or the other is expected, which can eventually lead to frustration and thereby to glassy features. In addition, frustration can arise due to the structural differences between the coexisting phases.

Figure 6 shows the $M(T)$ dependence, using $H = 0.2$ T in FC and ZFC modes for samples with $y \geq 0.3$. The difference between ZFC and FC data suggest that the ZFC state of the samples at low temperature is metastable, i.e. frozen. When the temperature is increased in the presence of a magnetic field, the system unblocks and the FM phase grows against the AFM-CO phase. We identify the temperature where the ZFC curve has a maximum derivative with a blocking temperature (T_B) which depends on the applied magnetic field. A similar behaviour was observed recently for $\text{La}_{5/8-y}\text{Pr}_y\text{Ca}_{3/8}\text{MnO}_3$ with $y = 0.4$ [11] and $y = 0.375$ [27]. In [11], it has been shown that the ZFC/FC difference and a characteristic dynamical behaviour can be accounted for well by proposing a temporal evolution of the relative fraction of the coexisting phases through a hierarchy of energy barriers, which only depend on the actual value of these fractions. This dynamic behaviour is attributed to phase competition rather than solely to magnetic interaction frustration, as happens in conventional spin glasses. The abrupt

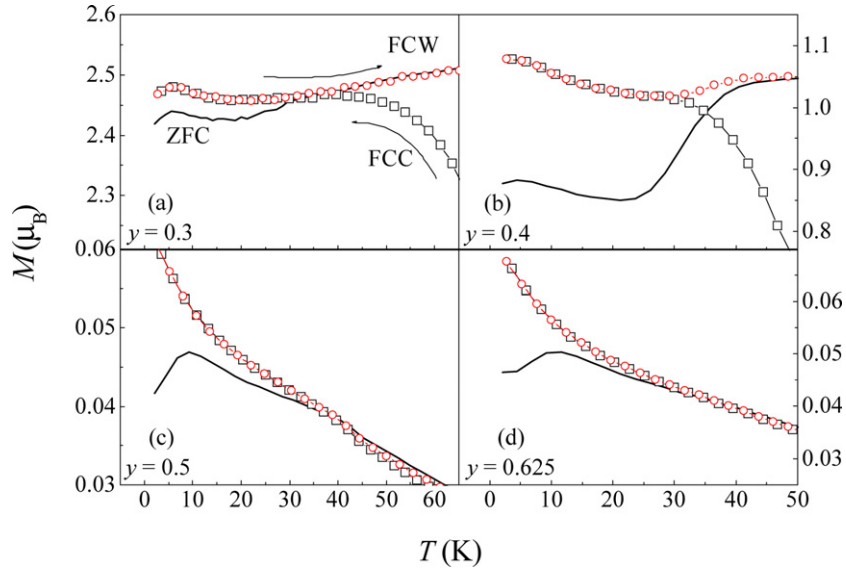


Figure 6. M versus T for $y = 0.3, 0.4, 0.5$ and 0.625 samples in the FC and ZFC modes. (This figure is in colour only in the electronic version)

metamagnetic transition observed for $y = 0.4, 0.5$ and 0.625 is also a signature that the systems are blocked at low temperature.

In figures 7(a) and (b) we show the dependence of T_B for $H = 0.2$ T and the difference $M_{FC} - M_{ZFC} = \Delta M_{FC-ZFC}$ measured at 2 K, respectively, as a function of Nd doping. Both variables exhibit a peak for $y = 0.4$. The blocking temperature can be regarded as a measure of the thermal energy needed for the system to overcome the energy barriers that separate the FM and AFM states; a larger T_B means higher barriers and thus a larger tendency to be blocked or ‘frozen’. On the other hand, ΔM_{FC-ZFC} measured at low temperatures is expected to be large when the system has a considerable volume fraction in the blocked regime. An interesting point is that a large value of T_B (large energy barriers) is correlated with a large ΔM_{FC-ZFC} (a large difference between the volume fractions in the blocked and nonblocked regimes). The maximum of both quantities near $y = 0.4$ is the signature of the enhanced blocked behaviour below T_B . It is worth noting that the existence of blocking temperatures is one of the most characteristic and intriguing features of phase-separated manganites [11, 27, 28].

The overall results that are presented can be summarized in the phase diagram displayed in figure 8. The filled symbols correspond to data obtained from $M(T)$ results while the empty symbols were obtained from $\rho(T)$. The magnetic transition temperatures obtained are in good agreement with those presented by Rao *et al* [14] and Moritomo [15], displaying the same overall tendency on doping, although in our case they are slightly smaller. Regarding Rao’s paper, the author has also observed a temperature corresponding to the change from insulator to metallic behaviour (T_p). Our results for T_p are shown in empty circles in figure 8. All samples are PI at high temperature. In the low Nd doping limit, the system undergoes a transition to the FM metallic state on cooling below 230 K. On doping, the system becomes less FM, as can be inferred from the reduction in T_C , and the CO state tendency is enhanced. These effects are due to the increase in the distortions of the Mn–O–Mn bond angles while reducing $\langle r_A \rangle$. At the other side of the diagram, the ‘pure Nd’ compound first becomes charge ordered at 225 K and, on further cooling, it orders antiferromagnetically ($T_N \sim 150$ K).

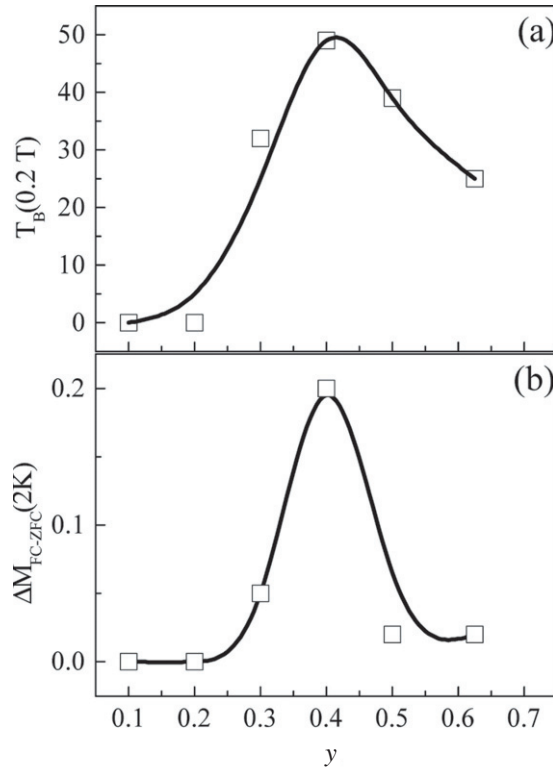


Figure 7. (a) Blocking temperature (T_B (0.2 T)) and (b) the difference of M_{FC} (2 K) and M_{ZFC} (2 K), as a function of doping.

In the intermediate doping region, limited by dashed lines, low-temperature data showed evidences of the phase-separated character of the samples. Within the PS regime, the change from insulator to metallic behaviour at T_p marks the limit between the temperature ranges in which the FM fraction may form percolative paths (percolative PS or PPS) or not (nonpercolative PS or NPPS) [14]. The existence of a blocked regime, enhanced around $y = 0.4$, shows that the phase coexistence at low temperatures is strongly affected by dynamical features of the phase-separated state, which allows the existence of frozen metastable states (frozen PS).

4. Conclusions

In conclusion, we performed magnetization and transport measurements on the $\text{La}_{5/8-y}\text{Nd}_y\text{Ca}_{3/8}\text{MnO}_3$ system in order to study the influence of the A-site mean ionic radius on the physical properties. The reduction in $\langle r_A \rangle$ inhibits the FM state, because it increases the number of distortions of the Mn–O–Mn bonds, and thus favours charge localization. The existence of a critical radius $\langle r_A \rangle \sim 1.18 \text{ \AA}$ where phase separation appears is evident, as previously observed in [19]. Our results show that the system is a paramagnetic insulator at high temperatures, while, on cooling, the ground state is FM metallic for low doping and AFM CO for high doping. For intermediate doping, there is a zone where the most stable state is phase separated. The change in the electrical transport behaviour from insulator to metallic shows the temperature below which the FM phase forms percolative paths through the sample.

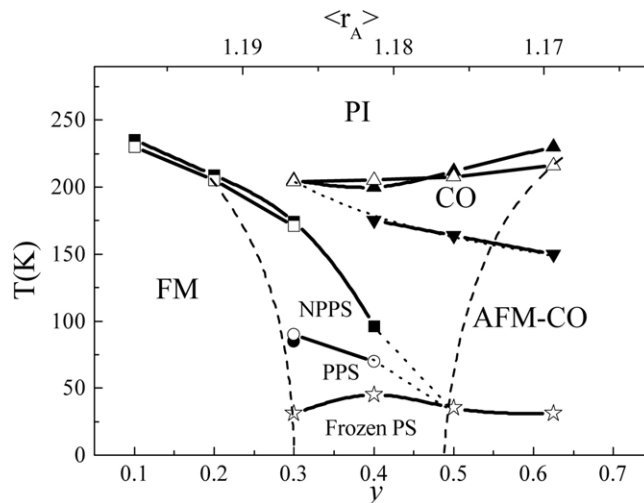


Figure 8. Electric and magnetic phase diagram of the LNCMO(y) system. Data of filled symbols are taken from $M(T)$ while empty ones are extracted from $\rho(T)$. The dashed lines mark the separation between being homogeneous and the PS state. Percolative PS (PPS) and nonpercolative PS (NPPS) stand for a state in which the FM metallic fraction form percolative paths through the sample or not, respectively.

The dashed lines in figure 8 mark the separation between homogeneous states and the phase separated state. According to recent theoretical developments, the origin of this window is closely related to the existence of disorder [12, 13]. In this case, disorder comes from the random distribution of the La and Nd ions on the A-sites. The presence of smaller Nd ions causes distortions of the Mn–O–Mn bond angle, which will be also disordered. These distortions can produce long-range deformations decaying as $1/r^3$, which trigger the clustering tendencies, leading to the formation of the phase-separated state [29]. A particular dynamical behaviour was also observed inside this window, characterized by the difference between the ZFC and FC curves, the existence of blocking temperatures and abrupt metamagnetic transitions. According to the particular phenomenology of phase-separated manganites, the competition between phases appears to be the cause of this behaviour. This dynamic phase-separated state was also theoretically proposed and the presence of disorder is believed to be the key for its existence [12, 13].

Acknowledgments

The authors thank M Quintero and L Granja for fruitful discussions. P Levy is a member of CIC CONICET. This work was partially supported by ANPCyT (PICT03-13517) and Fundación Antorchas (Argentina), and by CAPES, FAPERJ, and CNPq (Brazil).

References

- [1] Jin S, Tiefel T H, McCormack M, Fastnacht R A, Ramesh R and Chen L H 1994 *Science* **264** 413
- [2] Dagotto E, Hotta T and Moreo A 2001 *Phys. Rep.* **344** 1
- [3] Uehara M, Mori S, Chen C H and Cheong S-W 1999 *Nature* **399** 560
- [4] Mathur N D and Littlewood P B 2003 *Phys. Today* **56** 25
- [5] Uehara M and Cheong S-W 2000 *Europhys. Lett.* **52** 674

- [6] Kim K H, Uehara M, Hess C, Sharma P A and Cheong S-W 2000 *Phys. Rev. Lett.* **84** 2961
- [7] Dho J, Kim W S and Hur N H 2002 *Phys. Rev. Lett.* **89** 27202
- [8] Levy P, Parisi F, Granja L, Indelicato E and Polla G 2002 *Phys. Rev. Lett.* **89** 137001
- [9] De Teresa J, Ibarra M R, García J, Blasco J, Ritter C, Algarabel P A, Marquina C and del Moral A 1996 *Phys. Rev. Lett.* **76** 3392
- [10] Freitas R S, Ghivelder L, Damay F, Dias F and Cohen L F 2001 *Phys. Rev. B* **64** 144404
- [11] Ghivelder L and Parisi F 2005 *Phys. Rev. B* **71** 184425
- [12] Aliaga H, Magnoux D, Moreo A, Poilblanc D, Yunoki S and Dagotto E 2003 *Phys. Rev. B* **68** 104405
- [13] Dagotto E 2005 *New J. Phys.* **7** 67
- [14] Rao G H, Sun J R, Liang J K and Zhou W Y 1997 *Phys. Rev. B* **55** 3742
- [15] Moritomo Y 1999 *Phys. Rev. B* **60** 10374
- [16] Martín-Carrón L, de Andrés A, Ibarra M R, Zhao G-M and Martínez J L 2002 *J. Magn. Magn. Mater.* **242** 651
- [17] Sanjurjo J A, Granado E and Rettori C 2001 *J. Magn. Magn. Mater.* **226** 2000
- [18] Granado E, García A, Sanjurjo J A, Rettori C and Torriani I 2001 *Phys. Rev. B* **63** 64404
- [19] Sudheendra L and Rao C N R 2003 *J. Phys.: Condens. Matter* **15** 3029
- [20] Rivadulla F, López-Quintela M A and Rivas J 2004 *Phys. Rev. Lett.* **93** 167206
- [21] Schiffer P, Ramirez A, Bao W and Cheong S-W 1995 *Phys. Rev. B* **75** 3336
- [22] Jiráček Z, Krupicka S, Simsa Z, Dlouhá M and Vratislav S 1985 *J. Magn. Magn. Mater.* **53** 153
- [23] Dupont F, Millange F, de Brion S, Janossy A and Chouteau G 2001 *Phys. Rev. B* **64** 224403(R)
- [24] Levy P, Parisi F, Quintero M, Granja L, Curiale J, Sacanell J, Leyva G, Polla G, Freitas R S and Ghivelder L 2002 *Phys. Rev. B* **65** 140401
- [25] Sacanell J, Parisi F, Levy P and Ghivelder L 2004 *Physica B* **354** 43
- [26] Ghivelder L, Freitas R S, das Virgens M G, Continentino M A, Martinho H, Granja L, Quintero M, Leyva G, Levy P and Parisi F 2004 *Phys. Rev. B* **69** 214414
- [27] Wu W, Israel C, Hur N, Park S, Cheong S-W and de Lozanne A 2006 *Nat. Mater.* **5** 881
- [28] Sacanell J, Parisi F, Campoy J C P and Ghivelder L 2006 *Phys. Rev. B* **73** 14403
- [29] Burgoyne J, Moreo A and Dagotto E 2001 *Phys. Rev. Lett.* **92** 97202